JMEPEG (1997) 6:521-533

High-Temperature Performance Evaluation of a Directionally Solidified Nickel-Base Superalloy

D.A. Woodford and D. Stiles

The application of a new approach, design for performance, for high-temperature alloy development, design analysis, and remaining life assessment, based on short-time high-precision testing, is described in this paper. The material tested was a directionally solidified nickel-base alloy, GTD111. It was found that the creep strength at 850 °C was indeed superior to that of a competitive alloy, IN738, but was not necessarily enhanced by the preferred alignment of grain boundaries and crystal orientation. In contrast, the fracture resistance at 800 °C was improved in the longitudinal direction compared with transverse and diagonal orientations in terms of susceptibility to gas phase embrittlement (GPE) by oxygen. Specimens cut transversely and diagonally to the growth direction were more sensitive to GPE than specimens taken from conventionally cast IN738. The new conceptual framework allows account to be taken of GPE and other embrittling phenomena, which may develop in service, leading to rational life management decisions for gas turbine users. Additionally, straightforward design analysis procedures can be developed from the test data, which for the first time allow separate measurements of creep strength and fracture resistance to be used for performance evaluation.

Keywords creep, design, fracture, life prediction, stress relaxation

1. Introduction

Investment cast nickel-base alloys for hot section components of combustion turbines have evolved through improvements in chemistry and processing to a point where necessary property tradeoffs may preclude further significant advances in strength. For example, the classic conflict to optimize creep strength, fracture resistance, and environmental resistance may have been biased in recent years in favor of enhanced creep strength at the expense of fracture resistance (lower ductility and low cycle fatigue [LCF] life) and environmental resistance (increased reliance on coatings). For jet engine blades, during the last twenty years, the development of directional solidification and monocrystal technology, and associated chemistry modifications has allowed some improvements to be made in both creep strength and resistance to fracture because of the directional alignment or elimination of grain boundaries (Ref 1-3). This has presented a development opportunity for industrial gas turbines, and in recent years, directionally solidified blades have been offered to users in place of the large conventional castings (Ref 4).

Because of the different and widely varying operating conditions of the industrial gas turbine compared with the jet engine, it is appropriate to consider critically the use of a directionally solidified alloy for this application. The objective of directional solidification (DS) technology, in terms of previous studies, is summarized to identify the performance requirements for industrial gas turbine blades, review current design strategy, and propose an improved test methodology. The experimental section of this paper reports results of the GE alloy GTD111 (a modification of the aircraft engine blade alloy Rene 80) for various orientations and compares them with similar data for a well-established conventionally cast alloy, IN738.

Directional solidification produces a directionally aligned grain boundary morphology, results in sharp crystallographic texture and dendrite alignment, and may lead to reduced porosity with a generally more uniform precipitate distribution. Creep strength and fracture resistance are strongly sensitive to orientation in terms of both the crystallographic orientation and the grain boundary directionality. Early work showed an increased stress rupture life in the longitudinal direction for many alloys and a significant increase in tensile ductility. At the same time, transverse properties caused some concern because of the unfavorable alignment of the grain boundaries perpendicular to the applied stress for this case. In some alloys, it was necessary to add grain boundary tougheners, such as hafnium (Ref 5), to achieve acceptable transverse fracture resistance.

Because much of the enhanced rupture life in the longitudinal direction in DS alloys is due to increased ductility and prolonged tertiary creep, the rupture life can be a poor indicator of creep strength. For example, creep strength in directionally solidified IN738, defined in terms of time to strains up to 1.5% creep strain for temperatures between 800 and 1000 °C, was greater for specimens cut transverse and at 45° than for longitudinally oriented specimens (Ref 6). The General Electric design criterion for cast superalloys of time to 0.5% creep (Ref 7) makes better sense as a creep strength criterion than does time to rupture but may point to no clear advantage for this property from DS alloys. This design criterion stemmed from observations of environmentally enhanced surface cracking in conventionally cast alloys at about this strain, that is, the onset of fracture processes (Ref 8). The basis for the criterion can thus be inapplicable for DS material if cracking occurs at higher strains for specimens oriented in the longitudinal direction. The source of the difficulty is the continued attempt to use a deformation measurement as a basis for design against fracture.

The major advantage of a DS alloy appears to be the increased tensile ductility and the resultant increase in resistance

D.A. Woodford, Materials Performance analysis, Inc., Santa Barbara, CA 93101, USA; **D. Stiles,** VECO Corporation, Anchorage, AL 99519-6612, USA.

to thermal fatigue cracking. Thermal fatigue and isothermal LCF under strain control are also expected to benefit from the lower modulus in the longitudinal [001] direction, which results in a lower stress for the same strain (Ref 9, 10). However, this reduced modulus will be a detriment under stress control where the fatigue crack propagation rate increases as the modulus decreases (Ref 11).

Environmental attack resulting in intergranular penetration of gaseous species such as oxygen (Ref 12) and sulfur (Ref 13) is believed to be the principal cause of embrittlement of superalloys in service and of time-dependent intergranular fatigue crack propagation (Ref 14, 15). This is the major justification for a DS alloy in view of the virtual elimination of transverse grain boundaries for the longitudinal orientation. However, the aligned boundaries can lead to an especially vulnerable situation for transverse thermomechanical strains. For example, longitudinal splitting could occur from the blade tips or in cooling holes.

This brief outline does not address all the complexities or the many outstanding studies but attempts to identify the broad issues and some of the misconceptions. For example, DS technology is often promoted as giving increased creep life (referring to time to rupture). This is a meaningless term in a service context because the components do not typically creep more than a fraction of a percent, and as described above, there is no reason why the properly defined creep strength should be higher. Indeed, studies on monocrystals show that the [001] growth direction does not have the highest intrinsic creep strength (Ref 16, 17). Moreover, the structural and mechanical state of a superalloy in service changes as a function of blade location (differing thermomechanical exposures) as well as operating cycles, which are not adequately simulated in long time isothermal constant load creep tests. Because such tests also incorporate an arbitrary combination of deformation and fracture processes, service cracking and catastrophic failure of embrittled blades, not surprisingly, cannot be readily explained on the basis of available long time data. One final important criticism of the traditional approach is that material taken from a failed component will have a finite creep rupture life, and hence, the test cannot be used directly to predict part failure in unbroken components. This is the remaining life paradox (Ref 18).

To establish a sound conceptual basis for materials development component design, and remaining life assessment, a new approach, termed design for performance, was developed (Ref 19). Based on short-time high-precision tests, it allows separate measurements of creep strength and fracture resistance. By identifying minimum performance values for separate criteria, it is possible to use the same framework for initial material development and remaining life assessment. Rather than attempt to incorporate complex service-induced microstructural changes in the test methodology, in the new approach, the test is used to monitor the consequences of changes in terms of critical properties.

The creep strength criterion is obtained from a series of carefully conducted stress relaxation (SRT) tests (Ref 19, 20). The stress versus time response is converted to a stress versus creep strain-rate response. This is, in effect, a self-programmed variable stress creep test. Typically, a test lasting less than one day can cover five decades in creep rate. The accumulated inelastic strain is usually less than 0.1%, so that several relaxation runs at different temperatures and from different stresses can be made on a single specimen with minimal change in the mechanical state. Thus, an enormous amount of creep data can be generated in a short time.

A constant displacement rate (CDR) test (Ref 21), in which a crack is enabled to initiate naturally at a grain boundary and propagate slowly under closed-loop displacement control, was developed as a separate basis to evaluate fracture resistance. Both types of tests were first performed on large specimens to establish the broad principles of the methodology and then compared with data taken from miniature specimens machined from actual blades (Ref 22). It was established that environmental interaction, specifically gas phase embrittlement (GPE) resulting from intergranular penetration of oxygen, could drastically reduce the fracture resistance with little or no effect on the creep strength. The embrittlement was most pronounced at intermediate temperatures, that is, near 800 °C, for high strength cast superalloys.

This paper describes results from SRT and CDR tests on miniature specimens taken from a new directionally solidified Frame3 GE turbine blade (GE Company, GE Turbines, Schenectady, NY) made from directionally solidified and heat treated GTD111. The alloy is a derivative of Rene 80, a well-established jet engine blade alloy, and has comparable mechanical properties to that alloy. As far as is known, no additional compositional changes were made from the conventionally cast form of GTD111. Because this alloy has been in service for several years, and in some machines failures were reported, it is appropriate to develop a comprehensive mechanical characterization of the alloy. This includes an assessment of orientation effects and oxygen embrittlement effects for both creep strength and fracture resistance as functions of grain boundary orientation. These data are compared with similar results for conventionally cast IN738.

2. Experimental Procedure

2.1 *Material Specimen Dimensions*

Miniature specimens used in this study were designed to be machined from thin sections of gas turbine blades (Ref 20) and were 41 mm long with a reduced section of 32 by 1.9 mm. Six specimens were cut from the blade shank at each of three orientations: parallel, perpendicular, and at 45° to the growth direction. In addition, two specimens were taken from the trailing edge and one from the leading edge. For the CDR tests, the same small specimens were used.

Previously reported (Ref 20) SRT and CDR tests on conventionally cast IN738 are included for comparison.

2.2 *Stress Relaxation Testing*

The tests reported in the present paper, at a temperature of 850 °C, were loaded either at a stress rate of 10 MPa/s to a prescribed stress and then immediately transferred to strain control to hold the total strain on the specimen constant or were loaded at a constant strain rate of 0.01%/s to a set strain. With

the capacitive extensometer, this was maintained to $\pm 5 \times 10^{-6}$ for the test duration, which was usually one day.

The stress versus time response is converted to a stress versus creep strain-rate response by differentiating and dividing by the modulus measured on loading (Ref 19). The accumulated inelastic strain is usually less than 0.1%, so several relaxation runs at different temperatures and from different stresses can be made on a single specimen with minimal change in the mechanical state. Thus, an enormous amount of creep data can be generated in a short time. By appropriate cross plotting, pseudo stress-strain plots can be constructed and then used to generate strain versus time or stress versus time curves.

2.3 *Constant Displacement Rate Testing*

This test involved tensile testing to fracture at 800 °C under closed-loop strain control on the specimen. The temperature was chosen to be in the range of greatest susceptibility to gas phase embrittlement (GPE) (Ref 23), and the displacement rate was 1%/h. For the three orientations, the susceptibility to GPE by oxygen was evaluated in terms of high-temperature prior exposures in air and compared with similar data for IN738. As in previous studies (Ref 19, 20, 22), some exposures in vacuum were used for comparison. In this case, the samples were exposed at the same temperatures in evacuated quartz capsules.

3. Results

3.1 *Stress Relaxation Tests*

Figure 1(a-c) shows plots of stress versus natural logarithm time for the three specimen orientations. In these tests, the specimen was loaded at a constant stress rate, and for each orientation, all runs were on one specimen. This was justified on the basis that the proportional limit was the same for each test. For the test conditions, there was no significant change in mechanical state. The pattern of response is similar, including a clear tendency for the curves to cross at long times. This effect is also shown in Fig. 2(a-c), in which the stress versus strain-rate curves are plotted. The average value of the modulus was measured for these data as 91,600, 177,200, and 144,400 MPa for the longitudinal, diagonal, and transverse orientations, respectively. These curves are interesting in that a horizontal cut at a fixed stress below the crossover would predict higher creep rates at higher strains, that is, a concave upward initial creep transient. Conversely, a concave downward primary creep curve is predicted for stresses above the crossover. This behavior is often observed in standard creep tests.

Because of the lower modulus in the longitudinal orientation, the plastic strain on loading to the higher stresses is greater for the runs from the highest stresses, and the crossover of these curves is more pronounced (the creep rate at low stresses is higher). This crossover can have important consequences in service if local yielding occurs, for example, at stress concentrations on startup. Locally deformed material will have quite different creep properties from the surrounding undeformed material. Note that the lower stress curves are parallel and indicate different behavior if yielding does not occur. The upper limit for this behavior is for the relaxation run from 400 MPa for all orientations, and the curves from that stress represent a locus of microyield stress as a function of inelastic strain rate. Extrapolation of these curves approximately an order of magnitude lower in strain rate gives the stress for a creep strain of 0.5% in 50,000 h (3×10^{-11}/s). Thus, setting design stresses for isothermal uniaxial conditions could be based on a proportioning of this stress.

Figure 3(a-c) shows stress versus strain-rate curves for specimens loaded sequentially at fixed strain rates to total strains of 0.2, 0.4, 0.8, and 1.5%. The crossovers again are clear, and the curves show similar characteristics to those in Fig. 2. However, because of the lower modulus, the curve at 0.2% strain for the longitudinal specimen is lower. As with the other data, the 0.4% curve corresponding to the onset of plastic flow on loading appears to give a useful design locus for extrapolation. In this case, the average modulus values were 96,800, 177,300, and 137,000 MPa for the longitudinal, diagonal, and transverse. These are similar to those recorded for stress rate loading control.

A comparison of data on longitudinal specimens taken from the shank with those taken from the airfoil in Fig. 4(a, b) shows some variation for the 0.4% runs but a close response from 0.8%. This is consistent with minor differences in modulus and yielding and reflects the reality of how the creep properties can vary with location in the part.

Figures 5(a) and (b) show data comparison for both strain levels on several longitudinal specimens with those measured for the diagonal specimens, and Fig. 6(a) and (b) shows transverse specimens. Provided little or no plastic strain occurs during loading, the longitudinal orientation has lower creep strength at high stresses but higher creep strength at low stresses. For the 0.8% run, there is little choice among any of the specimens for all orientations.

Most of the previous testing on IN738 was limited to strains of approximately 0.2%, so comparisons with the GTD111 data were limited. Figure 7 shows that the average creep rate for a given stress, in comparison with transverse and diagonal specimens of GTD111, is approximately ten times higher for IN738 at 850 °C.

3.2 *Constant Displacement Rate Tests*

Figure 8 shows CDR results at 800 °C for the three GTD111 orientations compared with data on IN738 taken from a test slab casting using the same miniature specimens. All specimens show reasonable ductility at this intermediate test temperature. Although the yielding stresses are higher for GTD111 for all orientations, there is a pronounced fall in flow stress at higher strains for the transverse and diagonal orientation, below corresponding values for IN738. Pending further verification of this effect, no explanation is proposed.

To compare the effect of orientation on embrittlement by oxygen (GPE), specimens were exposed at 1000 °C for 24 h in air. In the longitudinal orientation, with very few grain boundaries intersecting the surface, the ductility was reduced by about 30% (Fig. 9). However, the other specimens failed with little or no plasticity. Figure 10 shows that, for the diagonal orientation, even 5 h exposure at this temperature leads to an appreciable loss in fracture resistance. This figure also shows that a specimen that had previously been exposed at 850 °C for a week of SRT testing was unembrittled.

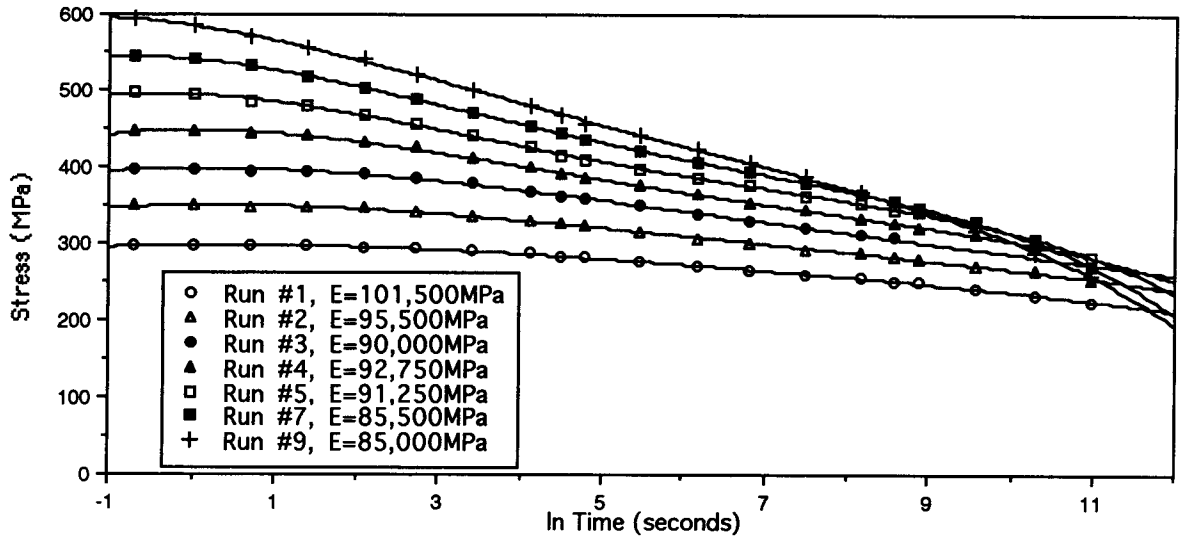

(a)

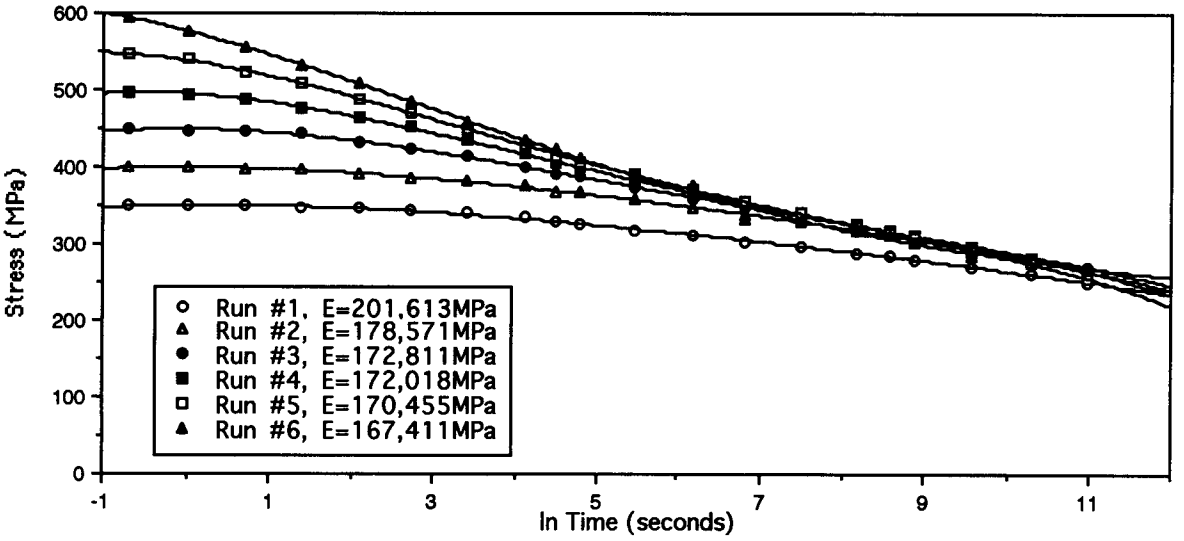

(b)

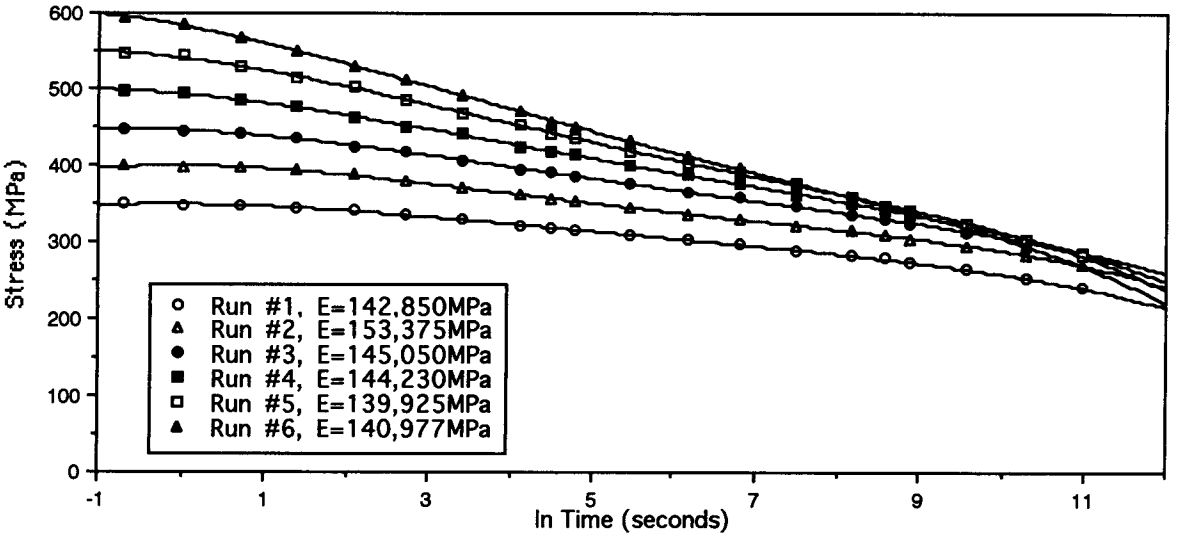

(c)

Fig. 1 Stress relaxation curves for (a) longitudinal orientation, (b) diagonal orientation, and (c) transverse orientation

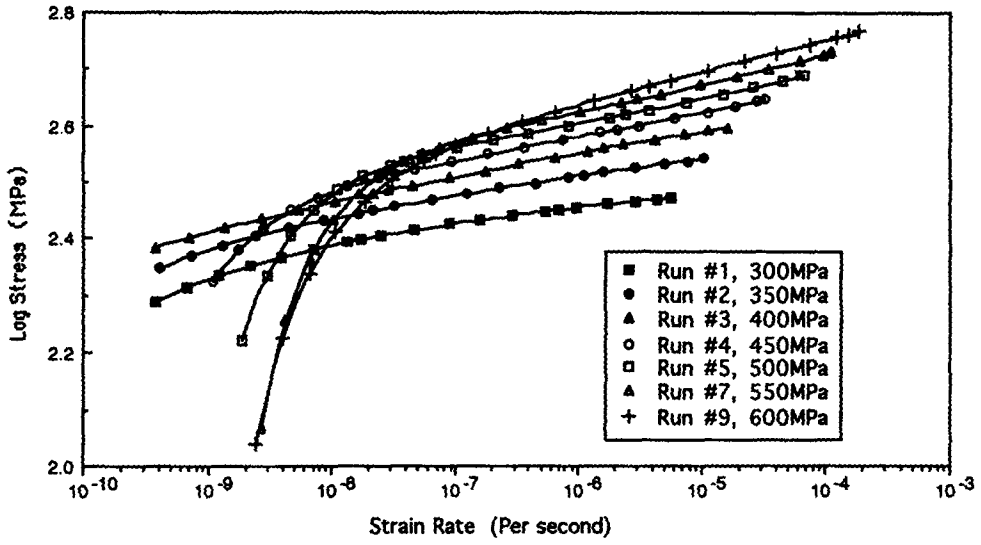

(a)

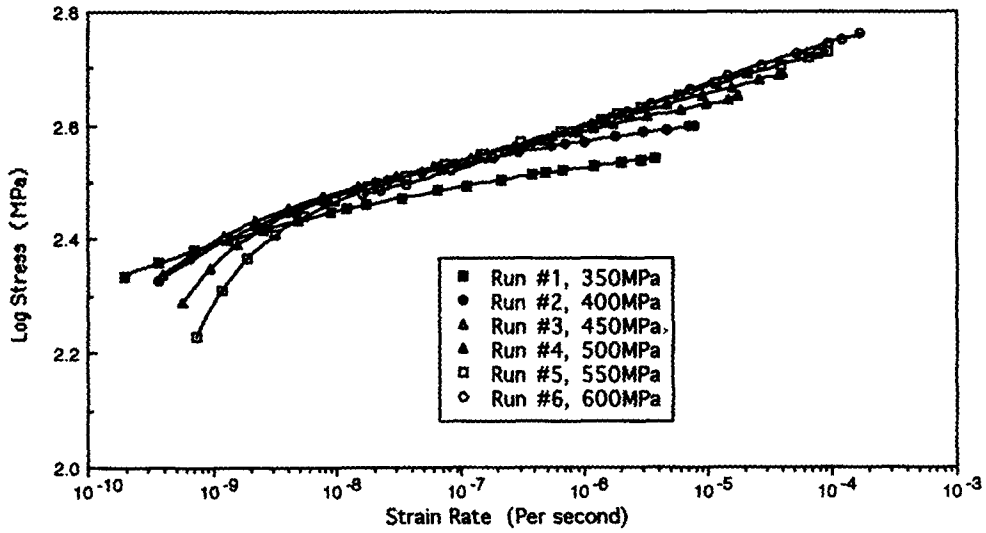

(b)

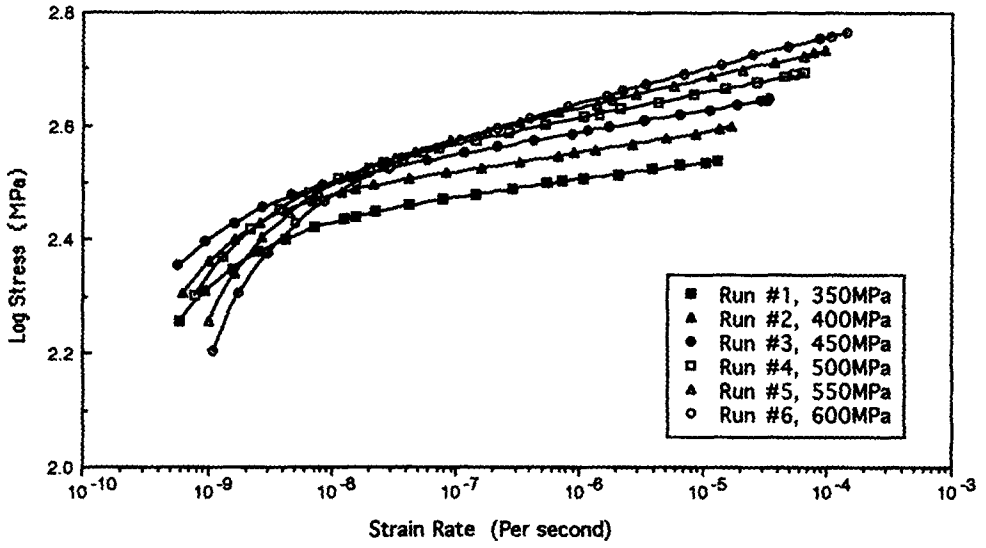

(c)

Fig. 2 Stress versus creep rate curves from various stresses for (a) longitudinal orientation, (b) diagonal orientation, and (c) transverse orientation

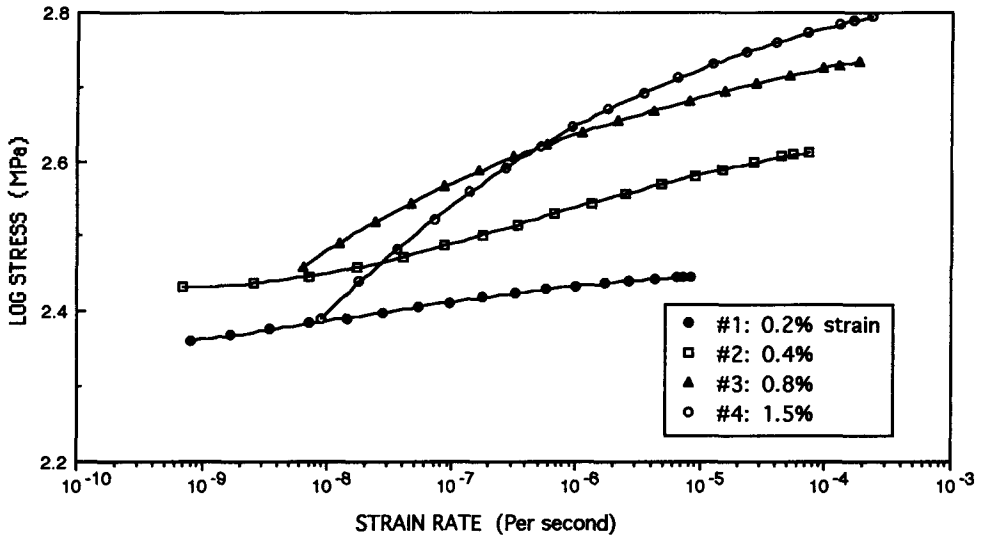

(a)

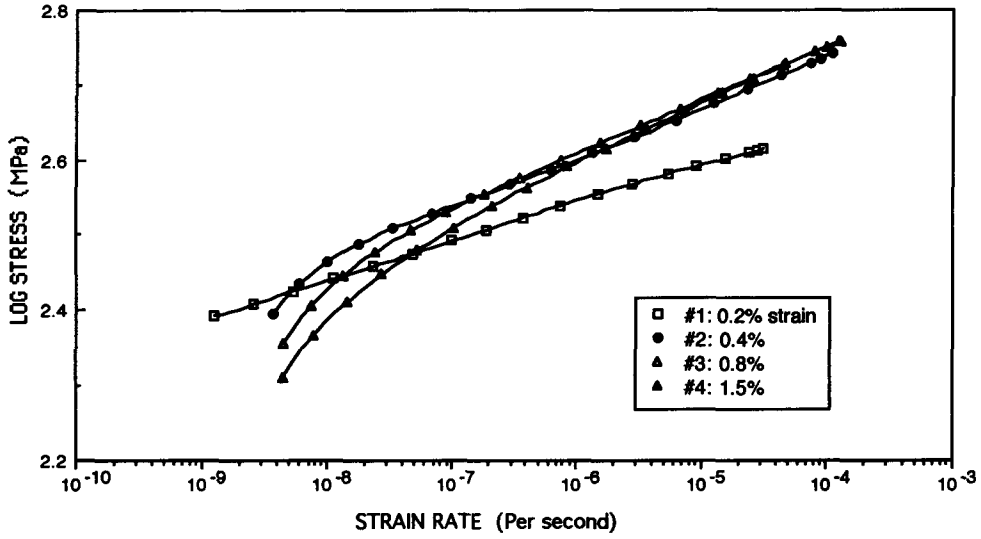

(b)

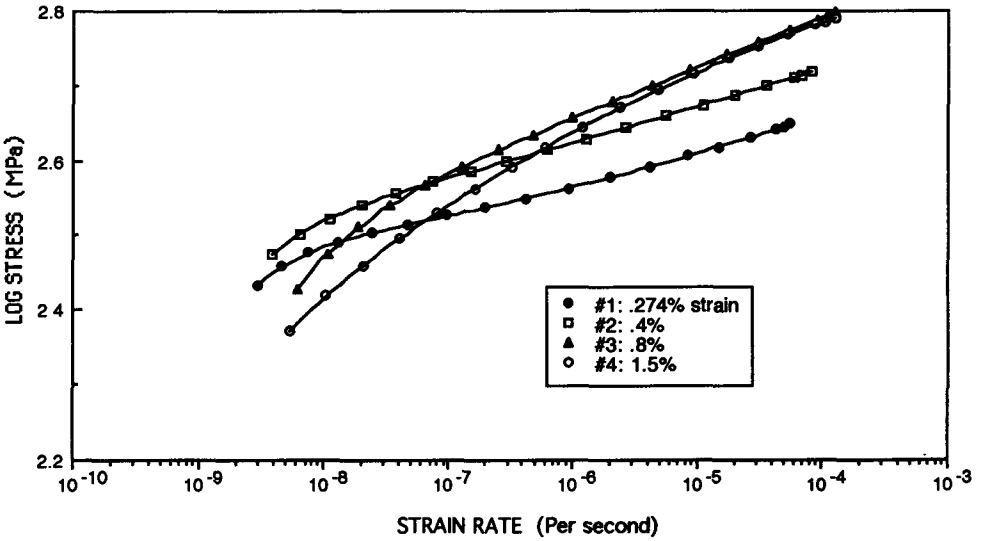

(c)

Fig. 3 Stress versus creep rate curves from selected strains for (a) longitudinal orientation, (b) diagonal orientation, and (c) transverse orientation

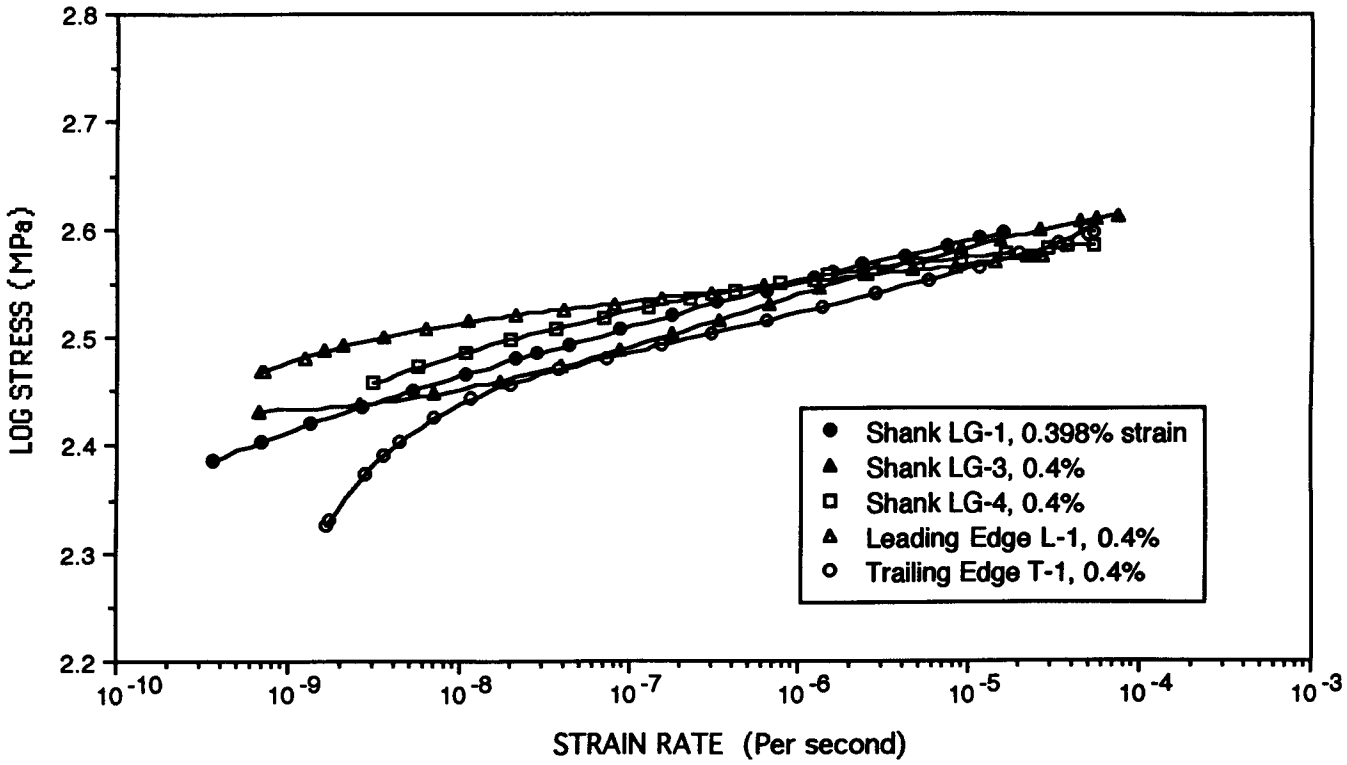

(a)

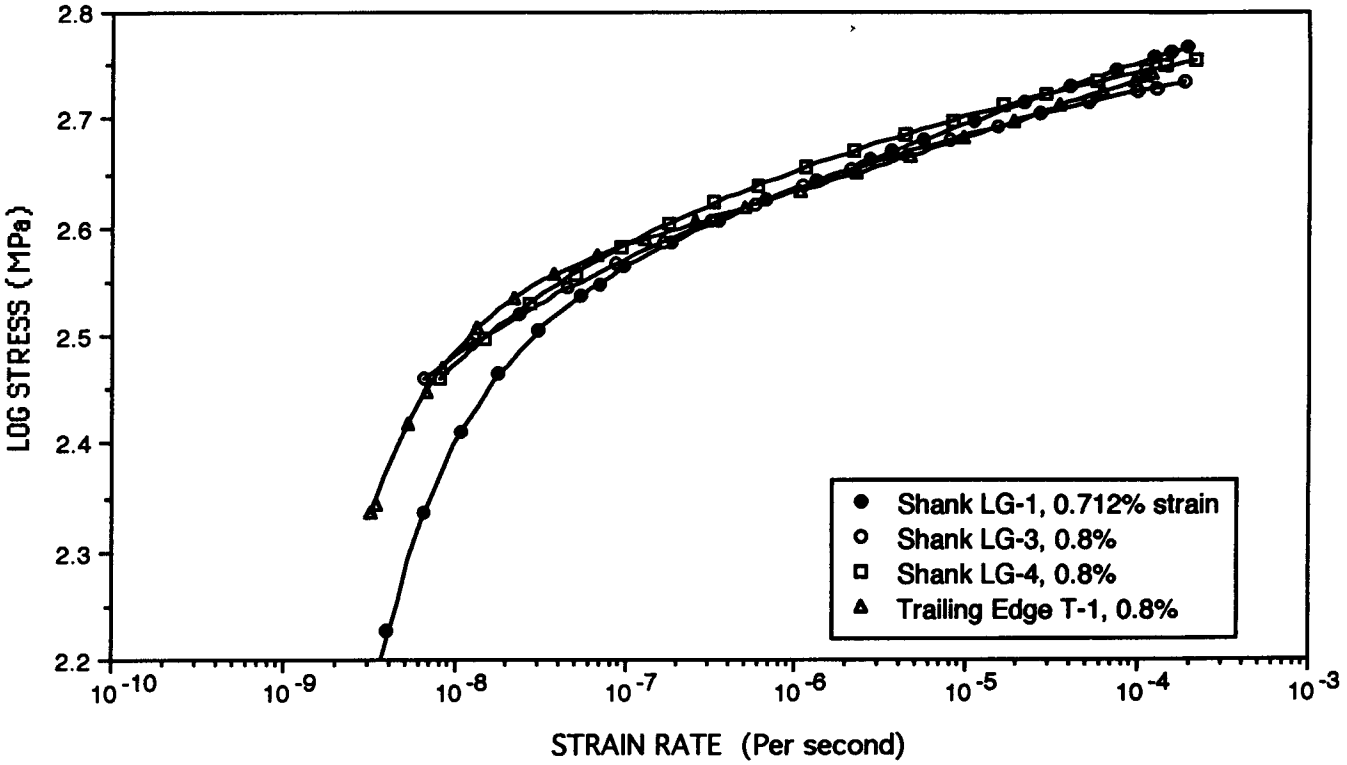

(b)

Fig. 4 Results of stress relaxation tests at 850 °C for longitudinal specimen. (a) 0.4% strain. (b) 0.8% strain

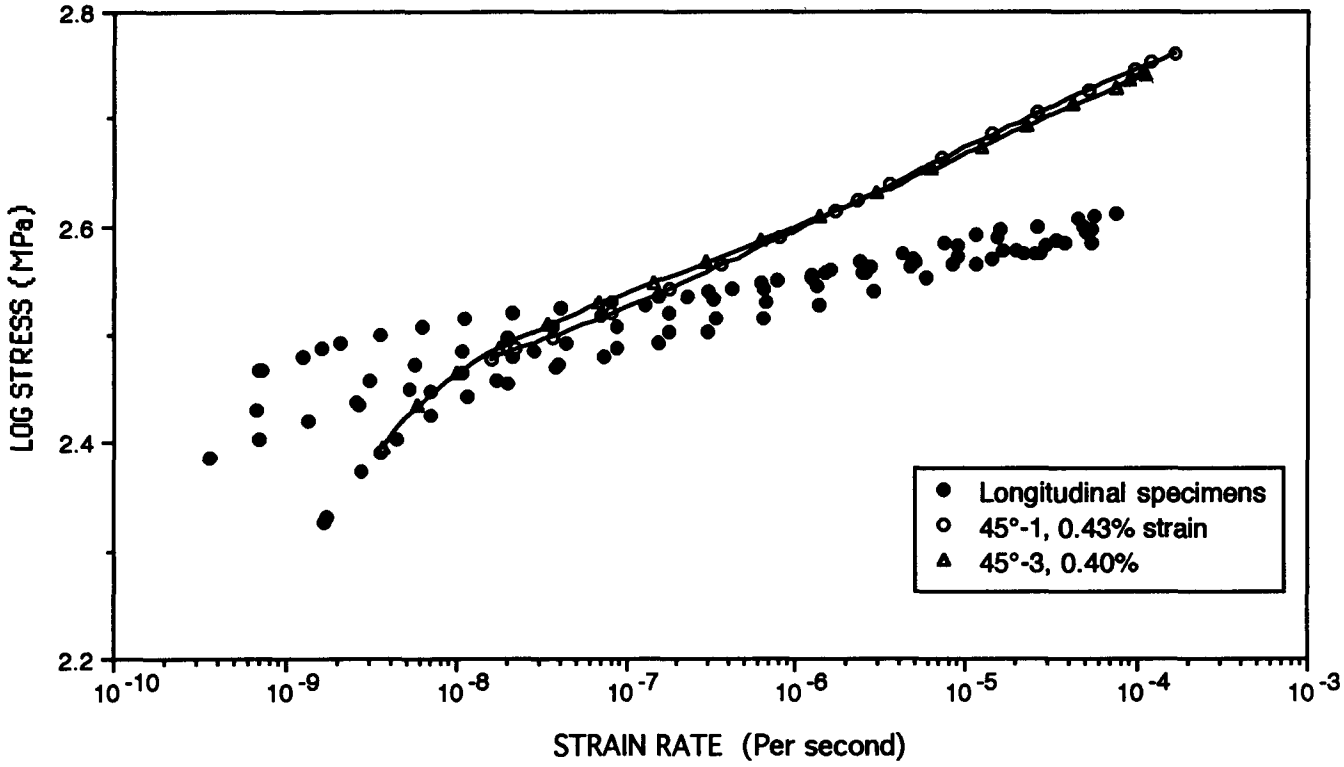

(a)

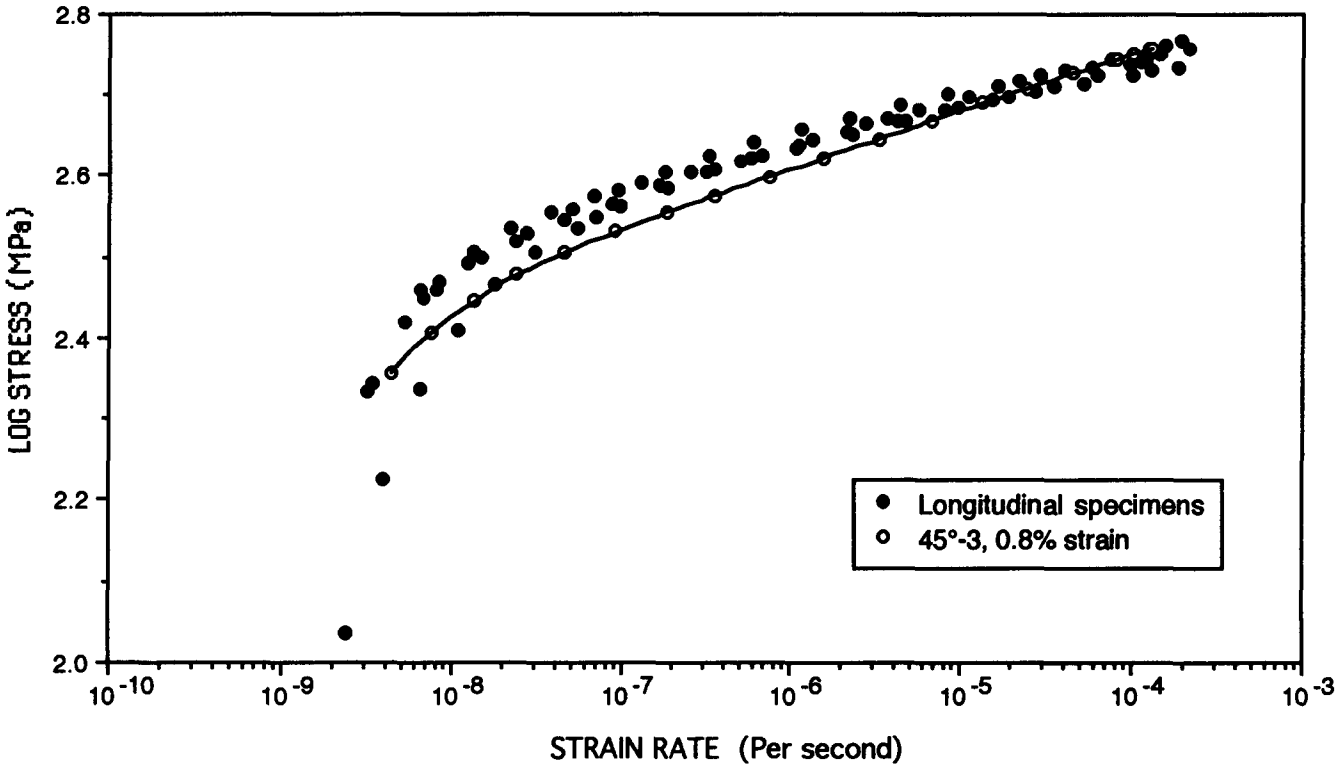

(b)

Fig. 5 Comparison of results for diagonal and longitudinal specimens. (a) 0.4% strain. (b) 0.8% strain

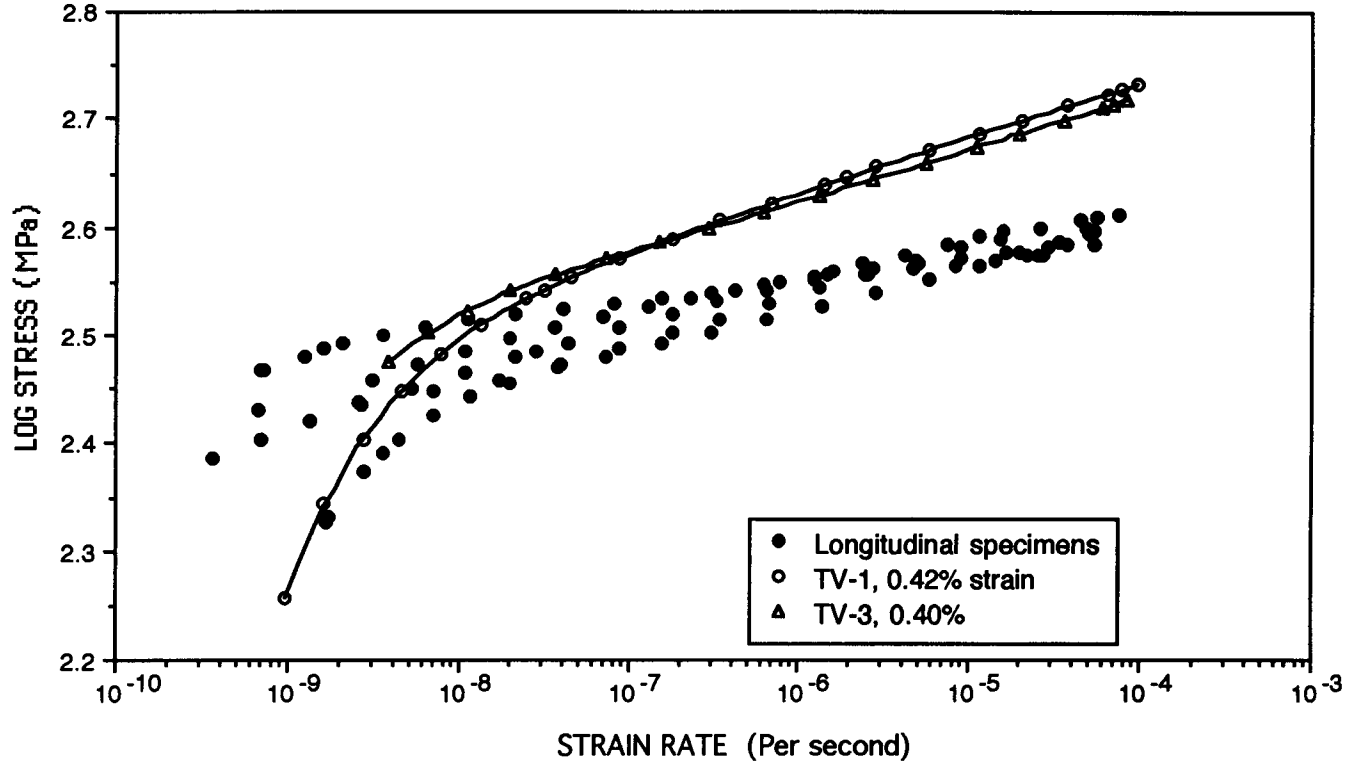

(a)

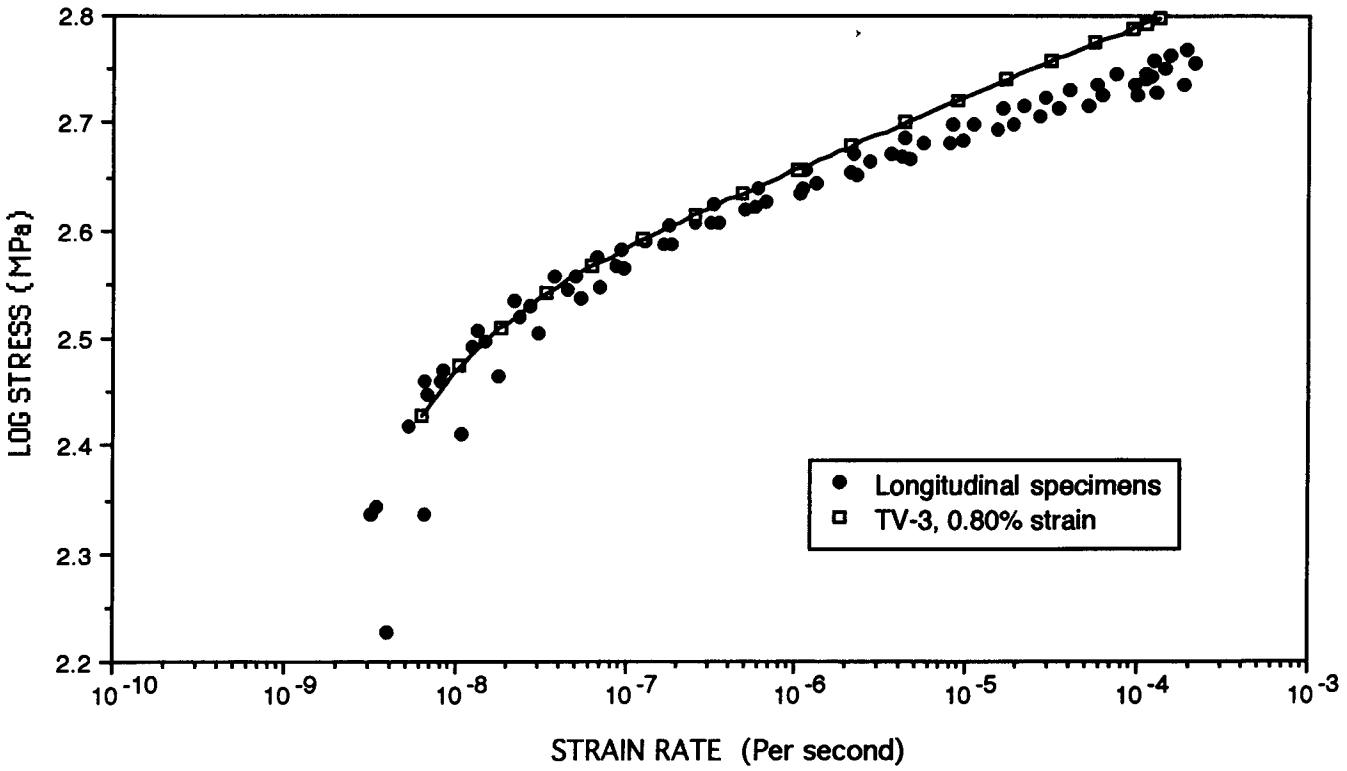

(b)

Fig. 6 Comparison of results for transverse and longitudinal specimens. (a) 0.4% strain. (b) 0.8% strain

Vacuum exposure at 1000 °C appears to be more harmful than air exposure in the longitudinal orientation (Fig. 11). Although vacuum exposures of large specimens have always protected against embrittlement (Ref 19), it is possible that the small amount of oxygen present after encapsulation can embrittle the miniature specimens. This example of embrittlement after vacuum exposure is confirmed by the data in Fig. 12 for transverse specimens. As before, exposure in SRT tests at 850 °C does not embrittle. Finally, Fig. 13 compares the embrittlement of GTD111 with previously published work on IN738 (Ref 20). Both alloys are strongly susceptible to GPE after this severe exposure. Consistent with its higher strength, GTD111 appears somewhat more prone.

4. Discussion

It has become increasingly clear that the traditional approach to materials development and design, involving long time creep testing, is not able to explain instances of part failure, especially for nickel-base superalloys operating under nonsteady conditions in aggressive environments. The new approach proposed here offers several innovations in concept: separation of creep strength and fracture criteria, short-time high-precision evaluation of the consequences of thermomechanical exposures, and setting limiting critical property values to establish unambiguously appropriate criteria for the end of part life.

Reported test data confirm a significant increase in creep strength for GTD111 compared with IN738 but find no clear advantage in the growth direction as a result of directional solidification. The apparent advantage at low strains for low strain rates (Fig. 5a, 6a) is a consequence of the lower modulus (e.g., for a fixed strain on loading, the starting stress is less), and there is less inelastic strain accumulated during relaxation for the longitudinal orientation. This advantage is not seen for tests started at a fixed stress (e.g., the runs from 400 MPa shown in Fig. 2 a-c). Thus, when comparing the creep strength for different orientations in anisotropic material, the effect of loading procedure must be recognized. No direct comparison has been made with conventionally cast GTD111.

The stress versus strain-rate curves readily provide a basis for alloy development and optimization of creep strength. They can also be used directly to set design stresses, possibly as outlined relative to the locus of microyield stress as a function of the strain rate. This can also be readily parameterized in terms of different test temperatures for aid in extrapolation, as described in Ref 19. If a more traditional representation is desired, one approach is to cross plot the data in terms of pseudo stress versus inelastic strain curves at fixed inelastic strain rates. Figure 14 shows a set of such curves. Normally, the designer can see similar curves crossplotted from creep curves at constant time intercepts to give isochronous stress versus strain curves. From curves, such as those shown in Fig. 14, creep curves can be constructed by taking horizontal sections at fixed stresses. At the intersection points, for the indicated strain, the time is calculated by dividing that strain by the inelastic strain rate. A more convenient approach may be to take a vertical cut so that a plot of stress versus time for a fixed creep strain can be plotted and extrapolated as desired. For example, Fig. 15

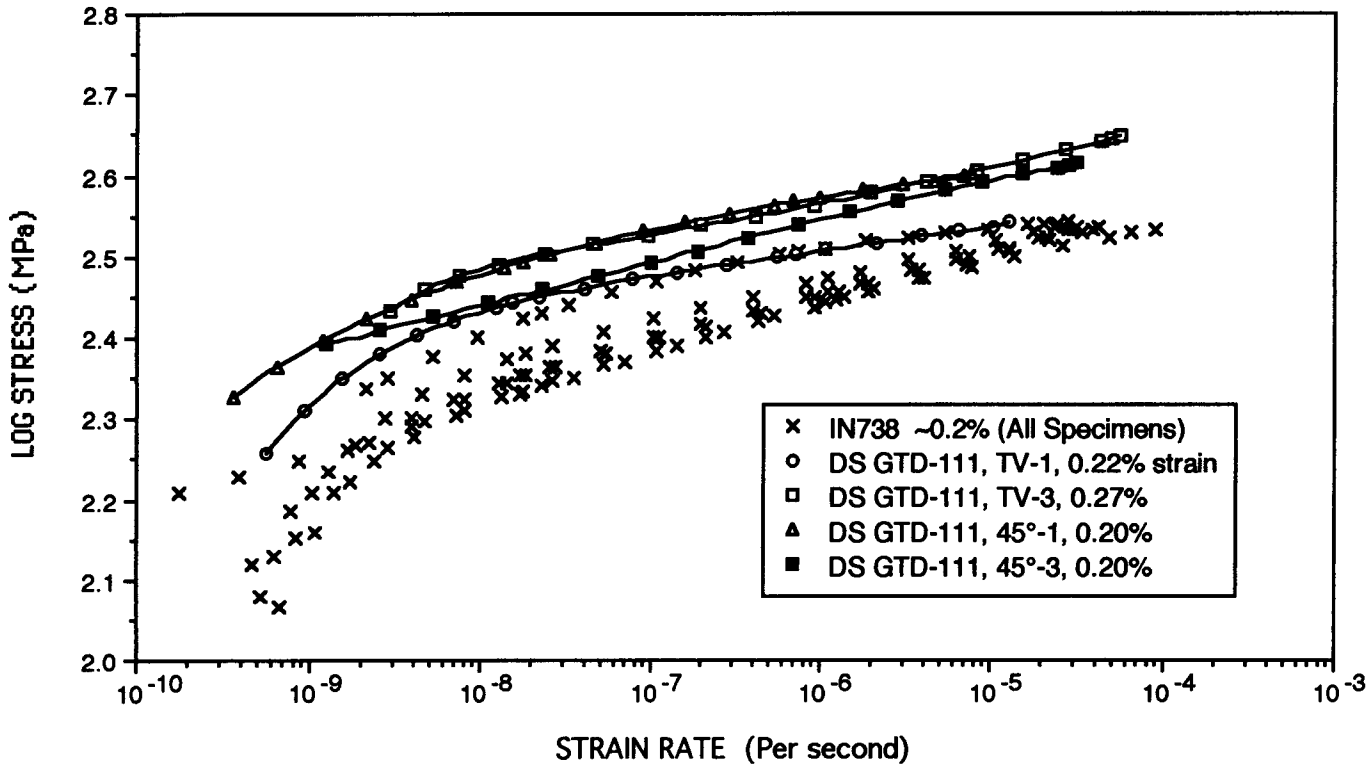

Fig. 7 Comparison of stress relaxation test results at 850 °C and 0.2% total strain between conventionally cast IN738 and DS GTD111 for transverse and diagonal specimens

shows a plot for the three orientations that is the same form which is often used to establish design stresses based on extrapolation of long time creep tests. It should be noted that these are methods to manipulate the relaxation data for presentation, and there is no intrinsic advantage in using any of these representations.

For cast superalloys, little effect of prior exposure, including 1000 °C treatments, has been observed for creep strength (Ref 19). Even a factor of five on creep rate may not have sufficient effect on stress to cause concern because of the strong stress dependence of creep rate. However, as reported (Ref 19, 20), a strong effect on fracture resistance based on the CDR test, especially from GPE, should create major concern. A suggested approach to quantifying this concern is to define a minimum acceptable CDR displacement at failure. For example, for the miniature specimens tested at 800 °C and 1%/h, this could be set at 0.5 mm. Anything less than that seems to indicate significant GPE. Additional refinements of such a failure criterion for service exposures can allow certain regions of the blade material to drop below this level, provided the bulk of the blade retained good fracture resistance. For example, trailing edge sections of a small IN738 blade were found to be the only region embrittled after 65,000 h service (Ref 20).

It is understood that fatigue failure involving both thermal and high cycle stress controlled processes can be involved in the initiation or propagation of a blade failure. However, when it is recognized that all monolithic materials (including polymers and ceramics) can be represented on unique curves for cyclic life (Ref 24) or crack propagation (Ref 11) for tests in an inert environment, the problem becomes clearly definable. Much routine and arbitrary air testing becomes unnecessary and can be misleading. Environmental interactions at the crack tip are the dominant factors influencing differences among materials, beyond the simple properties of strength, modulus, and ductility. When this is recognized, significant advances can be achieved (Ref 15) in quantifying in-service fatigue performance and optimizing alloy chemistry and processing for improved resistance to time-dependent fatigue crack propagation. At the present time, the proposed method of separately monitoring changes in a simple fracture criterion, in terms of sensitivity to environmental attack, is believed to be suitable and sufficient as a basis for establishing limiting performance criteria. Indeed, in the complex heating and cooling cycles of modern combustion turbines, maximum cyclic thermal strains can occur at intermediate temperatures in the cycle, exactly the range where the ductility is lowest (Ref 25) and where the fracture criterion is evaluated.

In response to service cracking in GTD111 blades, which has been associated with intergranular embrittlement, improved bilayer coatings have been introduced that should inhibit GPE (Ref 12). However, it is possible that the embrittlement observed after vacuum exposures, shown in Fig. 11 and 12, points to grain boundary segregation of embrittling species from the grain interior rather than from the external en-

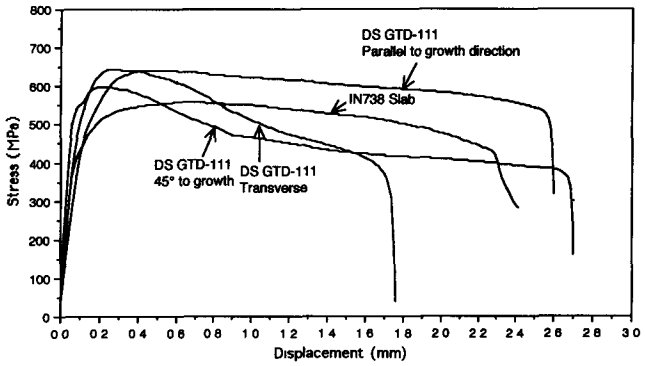

Fig. 8 Results of constant displacement rate tests at 800 °C on as-heat treated DS GTD111 and IN738

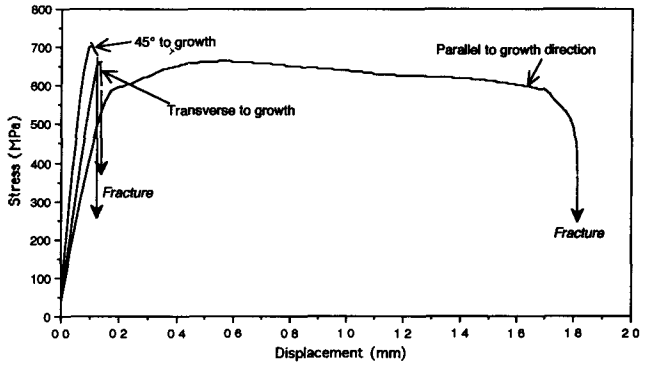

Fig. 9 Effect of exposure in air at 1000 °C for 24 h on constant displacement rate test results at 800 °C for the three orientations

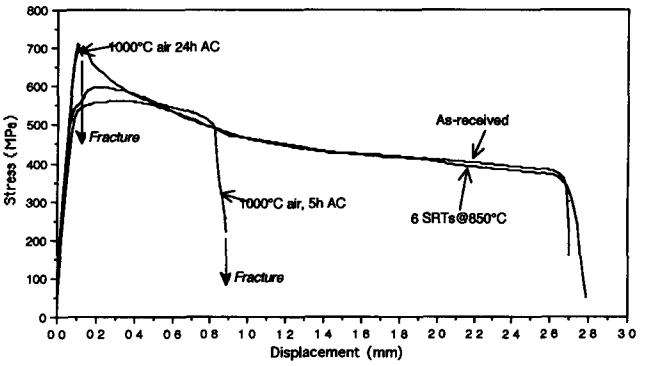

Fig. 10 Effect of various exposures on constant displacement rate tests at 800 °C for diagonal orientation

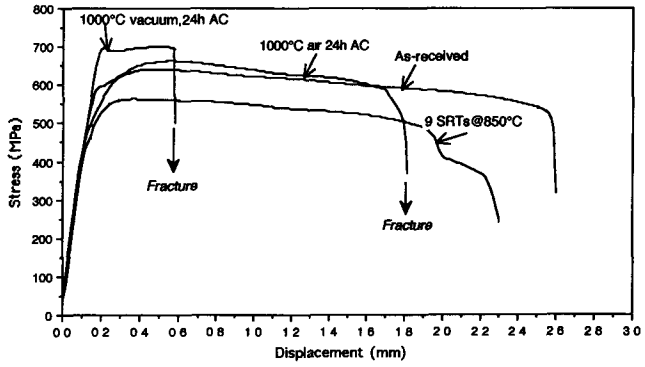

Fig. 11 Effect of various exposures on constant displacement rate tests at 800 °C for longitudinal orientation

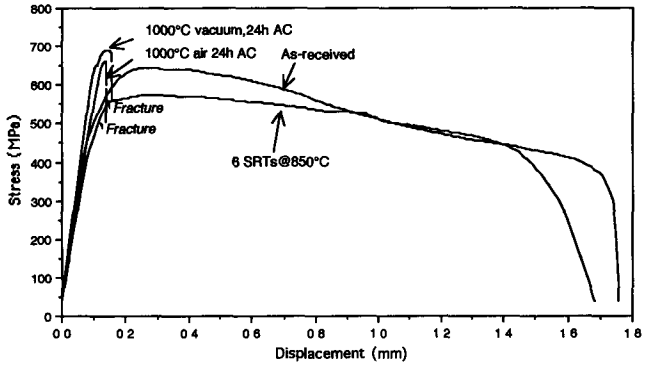

Fig. 12 Effect of various exposures on constant displacement rate tests at 800 °C for transverse orientation

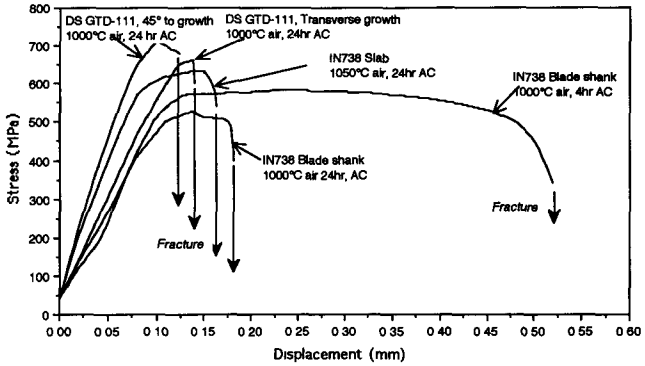

Fig. 13 Comparison of the effect on constant displacement rate test results of various air exposures on directional solidification GTD111 and IN738

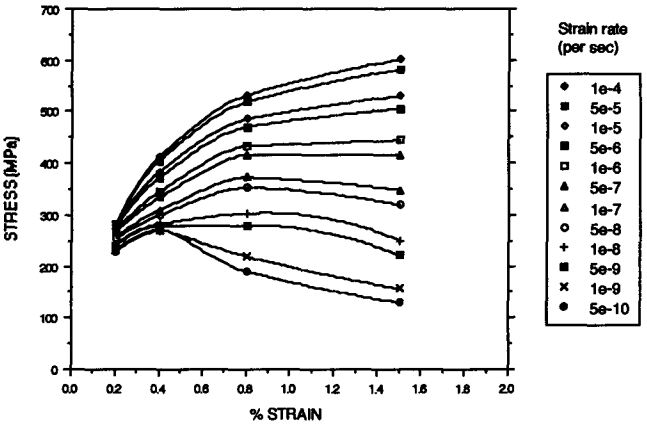

Fig. 14 Pseudo stress versus strain curves for various creep rates for a longitudinal specimen

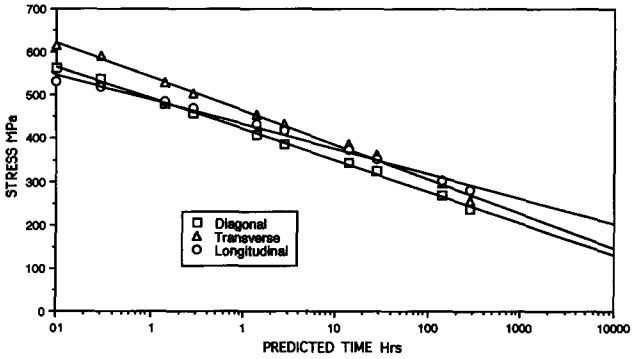

Fig. 15 Calculated stress for 0.5% creep strain versus time for the three orientations of DS GTD111 and 850 °C

vironment or to detrimental precipitation effects. The absence of strong getters for oxygen and sulfur, such as hafnium in GTD111, can exacerbate such segregation embrittlement. An examination of the microstructure using optical microscopy so far did not reveal anything of consequence. Fractures, in general, were interdendritic in the longitudinal specimens. For the other orientations, fractures were intergranular or, for two of the air exposed diagonal specimens, crystallographic. This latter observation was surprising and suggests that GPE can also occur on slip planes in these high strength alloys. Severe embrittlement in cast superalloys, except from GPE, was not previously observed. Even after vacuum encapsulation, there may be sufficient residual oxygen in the quartz capsule to embrittle the miniature specimens. This can be readily confirmed by comparing the effects of vacuum exposures of large specimens of GTD111 and miniature specimens of IN738. The recent service experience then must be explained on the basis of coating cracks breaking through to substrate grain boundaries or to slip planes. These cracks can be hairline and very difficult to detect. It is also conceivable that sufficient oxygen pickup occurs during the coating process and proceeds to diffuse into the thin sections during service. Finally, it should be noted that, at 1000 °C and higher, matrix diffusion rates are expected to approach grain boundary diffusion rates, which can account for the transgranular failures. This also suggests that eliminating all grain boundaries using monocrystalline technology might not eliminate this potential problem.

5. Conclusions

- A new design for performance methodology can be cheaper, faster, and fundamentally superior to traditional development and design procedures that are based on long time testing for high temperature applications.
- Based on this new approach, the superior creep strength of GTD111 compared with IN738 is readily confirmed. However, there appears to be no clear advantage in directional solidification for this alloy in terms of creep strength.
- Resistance to fracture, especially after high temperature exposure in air, is improved substantially for longitudinally oriented specimens of GTD111 compared with diagonal and transverse oriented specimens.
- When grain boundaries intersect the surface, GTD111 is more prone to GPE by oxygen than is IN738.
- Proposed design criteria for both creep strength and fracture resistance based on the new methodology can be used directly for life management of operating components.

Acknowledgments

This work was made possible by the financial support of ARCO Alaska. The authors are especially indebted to Donald Van Steele for all the detailed experimental work and to Kyle Amberge for writing the analysis programs and helping with data reduction and graphing.

References

1. F.L. Versnyder and R.W. Guard, *Trans. ASM,* Vol 52, 1960, p 485
2. B.H. Kear and B.J. Piearcey, *Trans. AIME,* Vol 239, 1967, p 1209
3. M. McLean, *Directionally Solidified Materials for High Temperature Service,* The Metals Society, 1983
4. P.W. Schilke, A.D. Foster, J.J. Pepe, and A.M. Beltran, *Adv. Mater. Process.,* Vol 4, 1992, p 22-30
5. J.S. Erickson, C.P. Sullivan, and F.L. Versnyder, *High Temperature Materials for Gas Turbines,* P.R. Sahm and M.O. Speidel, Ed., Elsevier, 1974, p 315-343
6. D.A. Woodford and J.J. Frawley, *Metall. Trans.,* Vol 5, 1974, p 2005-2013
7. G.T. Embley and V.V. Kallianpur, *Minnowbrook Conference on Life Prediction for High Temperature Gas Turbine Materials,* EPRI, 1985
8. W.L. Chambers, W.J. Ostergren, and J.H. Wood, *J. Eng. Mater. Technol.,* Vol 101, 1979, p 374-379
9. P.K. Wright and A.F. Anderson, *Superalloys 1980,* J.K. Tien, S.T. Wlodek, H. Morrow, M. Gell, and G. Maurer, Ed., American Society for Metals, 1980, p 8689-8698
10. D.A. Woodford, *Mechanical Behavior of Materials,* Vol 2, K.J. Miller and R.F. Smith, Ed., ICM 3, Cambridge, England, 1979, p 33-42
11. M.O. Speidel, *High Temperature Materials in Gas Turbines,* P.R. Sahm and M.O. Speidel, Ed., Elsevier, 1974, p 207-255
12. D.A. Woodford, *Metall. Trans. A,* Vol 12, 1981, p 299-308
13. J.P. Beckman and D.A. Woodford, *Metall. Trans. A,* Vol 21, 1990, p 3049-3061
14. D.A. Woodford and R.H. Bricknell, *Embrittlement of Engineering Alloys,* C.L. Briant and S.K. Banerji, Ed., Academic Press, 1983, p 157-196
15. K.-M. Chang, M.F. Henry, and M.G. Benz, *JOM,* Vol 42 (No. 12), 1990, p 29-35
16. R.A. McKay, R.L. Dreshfield, and R.D. Maier, *Superalloys 1980,* J.K. Tien, S.T. Wlodek, H. Morrow, M. Gell, and G. Maurer, Ed., American Society for Metals, 1980, p 385-394
17. P. Caron, Y. Ohta, Y.G. Nakagawa, and T. Khan, *Superalloys 1988,* D.N. Duhl, G. Maurer, S. Antolovich, C. Lund, and S. Reichman, Ed., The Metallurgical Society, 1988, p 215-224
18. D.A. Woodford, *International Conference on Fossil Power Plant Rehabilitation,* ASM International, 1989, p 149-154
19. D.A. Woodford, *Mater. Des.,* Vol 14 (No. 4), 1993, p 231-242
20. D.A. Woodford, D.R. Van Steele, K.J. Amberge, and D. Stiles, *Materials Performance, Maintenance and Plant Life Assessment,* I. LeMay, P. Mayer, P.R. Roberge, and V.S. Sastry, Ed., Met. Soc. Canadian Institute of Metals, 1994, p 85-100
21. J.J. Pepe and D.C. Gonyea, *International Conference on Fossil Power Plant Rehabilitation,* ASM International, 1989, p 39
22. D.A. Woodford, D.R. VanSteele, and D. Stiles, *EPRI Conference on Turbine Generators,* (Albany, NY), 1993
23. W.H. Chang, *Proceedings Second International Conference on Superalloys,* TMS-AIME, 1972
24. L.F. Coffin, *Creep-Fatigue-Environmental Interactions,* R.M. Pelloux and N.S. Stoloff, Ed., AIME, 1980, p 1-23
25. D.A. Woodford and D.F. Mowbray, *Mater. Sci. Eng.,* Vol 16, 1974, p 5-43